Model of metallic cohesion: The embedded-atom method

Murray S. Daw
Sandia National Laboratories, Livermore, California 94550
(Received 15 August 1988)

The embedded-atom method (EAM) [Phys. Rev. B **29**, 6443 (1984)] has proven to be a significant improvement in simplified total-energy calculations for metallic systems. In the current work, the ansatz used in the EAM is derived from the local-density functional for the energy. The expression demonstrated here is most appropriate for simple metals and for transition metals with nearly empty or nearly full *d* bands. An embedding energy is defined as a function of an optimal constant background density, and an equation for that optimal background density is obtained. The cohesive energy is then related to the embedding energy and an electrostatic two-body interaction. It is shown that lowest-order electronic relaxations can be absorbed into the same ansatz. Model calculations are presented for fcc nickel within the Thomas–Fermi–Dirac–von Weizsäcker model for the kinetic energy, with local exchange and correlation and frozen-electron distributions. The model is shown to provide a good description of the ground-state properties of nickel (e.g., energetics and structure of vacancies and surfaces) and also a good framework for evaluating the approximations used in justifying the EAM form. In particular, the model exhibits a simple relationship between the optimal constant background density and the background density at the atomic site. Corrections involving the gradient of the background density are shown to be important in the calculation of the surface energy. This work then provides a basis for the use of the EAM in semiempirical applications.

I. INTRODUCTION

The theoretical investigation of the structure and ground-state properties of complex metallic systems, until recently, relied almost exclusively on the use of interatomic pair potentials.[1] In the pair-potential scheme, the cohesive energy of a solid is given by a sum over pair bonds, plus a volume-dependent energy (or an energy dependent on some background electron-gas density). Using pseudopotential theory, a perturbation series can be set up which expresses the energy of the solid in successively higher powers of the scattering.[2] This systematic derivation shows how the interaction of atoms in jellium can be expressed in terms of a one-body (or density-dependent) interaction as well as the two-body and higher interactions. These interactions are dependent on the background electron-gas density, which could alternatively be viewed as being determined by the volume. From a phenomenological point of view, the one-body interaction is *required* in addition to the two-body interactions in order to describe the elastic properties of the solid.[3] However, the interatomic–pair-potential approach presents the problem of defining, in an arbitrary situation, the local electron density or the volume on an atomistic scale.

The use of interatomic pair potentials suffers from the neglect of many-body interactions, which obviously play a role in many interesting physical phenomena. For example, the presence of impurities must affect the metal-metal bond strength, involving an inherently many-body effect.[4] Similarly, two impurities in a metal interact through the host via a many-body interaction.[5,6] The intrinsic nature of the two-body approximation makes suspect the application of pair potentials to interesting defects.

Daw and Baskes[7] have proposed recently a new framework for calculating the energetics of metals, which they call the embedded-atom method (EAM). In this approach, the energy of the metal is viewed as the energy to embed an atom into the local electron density provided by the remaining atoms of the system. In addition, there is an electrostatic interaction. The ansatz that they used is

$$E_{\rm coh}=\sum_i F_i\left[\sum_{j\ (\neq i)}\rho_j^a(R_{ij})\right]+\tfrac{1}{2}\sum_{\substack{i,j\\(j\neq i)}}\phi_{ij}(R_{ij})\ , \qquad (1)$$

where F is the embedding energy, ρ^a is the spherically averaged atomic density, and ϕ is an electrostatic, two-body interaction. The background density for each atom in Eq. (1) is determined by evaluating at its nucleus the superposition of atomic density tails from the other atoms. Equation (1) combines the computational simplicity needed for defects and amorphous systems with a physical picture which includes many-body effects and avoids the ambiguities of the pair-potential scheme. This method has been applied successfully to such problems as phonons,[8] liquid metals,[9] defects,[7] alloys,[10] impurities,[7] fracture,[11] surface structure,[12,13] surface adsorbate ordering,[6,13] surface segregation,[14] surface order-disorder transitions,[15] surface ordered alloys,[16] and surface phonons.[17] The computer time required for the EAM is not significantly more than that required for pair-potential calculations.

The EAM ansatz was preceded by the independent work of Nørskov and Lang (effective medium[18]) and of Stott and Zaremba (quasiatom[19]). Nørskov and Lang showed that the heat of solution of a light, interstitial impurity (H and He, in particular) in metals could be calculated by replacing the host with a suitable effective medium, which in this case was jellium. Nørskov and his coworkers have had great success in calculating from first principles the heats of solution[20] and heats of chemisorption[21] of hydrogen in metals, the primary information being the energy gained by putting a hydrogen atom into jellium (i.e., the embedding energy). The optimal density of the jellium was determined by weighting the background metallic density by the Hartree potential of the metal ion. Stott and Zaremba arrived at a similar concept, based on viewing the impurity as a quasiatom in a nearly uniform electron gas.

Daw and Baskes[7] made a significant generalization with the EAM by proposing to view the cohesive energy of a metallic solid as comprised of the embedding energy plus electrostatic interactions. In this view, each atom in the metal is embedded into the electron gas created by the other atoms. Atoms near a defect such as a surface are embedded into an electron gas of different profile than atoms in the bulk. The process of embedding each atom is made symmetrical, so that the cohesive energy is manifestly symmetrical in the atomic index. They suggested the ansatz which will be discussed here. They then obtained the functions empirically by fitting to properties of the bulk metals. The generality of the functions was tested by applying them to surfaces and other defects. This generalization allowed calculations of complex metallic structures to be done within the approximate embedding-energy framework. The EAM incorporated significant many-body interactions, but the complexity of the calculation was no worse than the traditional two-body potentials. The EAM has thus become a popular replacement for interatomic pair potentials in the calculation of metallic defects.

Even more recently, Jacobsen, Nørskov, and Puska,[22] Manninen,[23] and Kress and DePristo[24] reexamined the ansatz used in the EAM with arguments based on the effective-medium approach. Jacobsen *et al.* demonstrated how the cohesive energy of a metallic system could be related to the embedding energies, with corrections accounting for the d-d hybridization in the transition metals. Their approach showed that with the neglect of the d-d hybridization (valid for simple metals and also presumably for early and late transition metals), the EAM expression is recovered. The density of the effective medium was taken to be an unweighted average of the background density over the Wigner-Seitz cell of the atom. Kress and DePristo suggested using as a weighting function the electron density of the atom itself, so that the background density is related to the overlap of charge densities. A correction to the embedding function based on a local-energy functional was used in their corrected effective-medium method to correct for inaccuracies in the definition of the optimal effective-medium density.

In this paper we show an alternative means of relating the cohesive energy to embedding energies. The approach is valid for systems where the kinetic, exchange, and correlation energies can be well approximated by a semilocal functional, and the electron density in the solid is not far from a linear superposition of single-atom densities. We expect therefore that the result is justified for systems where the d-d hybridization is negligible. The result is a definition of the embedding function, electrostatic contribution, and optimal electron density. The derivation is performed first assuming that the electron density in the solid is given by a superposition of atomic densities; then the same form is shown to hold to lowest order in the electron redistribution. The advantage of the current approach is that the approximations in the derivation can be tested within a model energy functional. We therefore set up a model energy functional for fcc Ni, based on the Thomas–Fermi–Dirac–von Weizsäcker (TFDvW) kinetic-energy functional and assuming a superposition of atomic densities. We then calculate the energetics of defects in Ni, such as vacancies and surfaces, and show that they agree well with experiment. Then we obtain the EAM functions directly from the model energy functional, and show that the resulting EAM energy faithfully approximates the energetics calculated from the model energy functional. Finally, we show how these EAM functions obtained from the TFDvW model are very similar to the earlier, semiempirical EAM functions.

This paper is organized as follows. In the Sec. II the EAM ansatz is derived from approximations to the density functional for the energy. In Sec. III we present the model energy functional for Ni, and defect calculations based on this model are described. Embedded-atom functions are obtained from the functional and applied to the same defect calculations. Here the approximations in Sec. II are tested and shown to be valid. The last section contains some concluding remarks.

II. DERIVATION

Our goal is to derive an approximate expression for the cohesive energy of a metallic system which is an explicit function of the positions of the atoms and which is simple to evaluate. To do this, we will start with the electron density of the solid, $\rho(r)$, and the energy functional of the electron density, $E[\rho]$.[25] We will assume that the kinetic, exchange, and correlation contributions to the energy, $G[\rho]$, are semilocal:

$$G[\rho]=\int d\mathbf{r}\,\gamma(\rho(r),\nabla\rho(r),\nabla^2\rho(r),\ldots)\ , \tag{2}$$

where the integral is understood here and elsewhere to be over real space. In what follows, we will rely on its semilocal nature by dividing G into a sum of contributions from individual volumes. We will abbreviate the function $\gamma(\rho(r),\nabla\rho(r),\nabla^2\rho(r),\ldots)$ by simply $g(\rho(r))$, keeping in mind that γ is also a function of the derivatives of the density. The cohesive energy of a solid is then

$$E_{\rm coh}=G[\rho]+\tfrac{1}{2}{\sum_{ij}}'\frac{Z_iZ_j}{R_{ij}}-\sum_i\int d\mathbf{r}\frac{Z_i\rho}{|\mathbf{r}-\mathbf{R}_i|}+\tfrac{1}{2}\int d\mathbf{r}\int d\mathbf{r}_2\frac{\rho(\mathbf{r}_1)\rho(\mathbf{r}_2)}{r_{12}}-E_{\rm atoms}\ , \tag{3}$$

where the sums over i and j are over the nuclei of the solid, the prime on the summation indicates omission of the $i=j$ term, and Z_i and $\mathbf{R}_i$ are the charge and position of the ith nucleus. Starting with Eq. (3), we will make the approximation that the charge density in the solid is only slightly different than a superposition of the atomic charge densities. This approximation is reasonable provided that covalent bonding in the metal of interest is negligible. We will therefore consider the derived equations to be valid only for simple metals and for early or late transition metals. The case of approximately half-filled d bands must be treated elsewhere.

We will now give a heuristic derivation of the EAM from Eq. (3). First, in Sec. II A the derivation assumes that the charge density in the solid is exactly a superposition of the atomic charge densities. The embedding energy is defined and the equation for the optimal background density is derived. In Sec. II B we extend the proof to include lowest-order relaxation in the charge density. In Sec. II C the equation for the optimal background density is examined, including the limiting case generally assumed in the EAM. In Sec. II D, a different grouping of terms in the energy gives an alternate, though equivalent, definition of the embedding function which is often used in practice. In Sec. II E we summarize the derivation.

A. Derivation using linear superposition of densities

In order to make Eq. (3) useful, we will express the electron density ρ explicitly in terms of the positions of the nuclei. We start by assuming that the electron density of the solid can be described as a linear superposition of the densities of the individual atoms $[\rho_s(r)\equiv\sum_i\rho_i^a(r-R_i)]$. The effect of charge redistributions will be considered in Sec. II B. Substituting $\rho(r)=\rho_s(r)$ into Eq. (3) gives

$$E_{\rm coh}=G\left[\sum_i\rho_i^a\right]-\sum_i G[\rho_i^a]+\tfrac{1}{2}{\sum_{ij}}'U_{ij}^a\ , \tag{4}$$

with

$$U_{ij}^a\equiv\int d\mathbf{r}_1\int d\mathbf{r}_2\frac{n_i^a(\mathbf{r}_1)n_j^a(\mathbf{r}_2)}{r_{12}}$$

and

$$n_i^a(r)\equiv\rho_i^a(r-R_i)-Z_i\delta(r-R_i)\ .$$

The first two terms in Eq. (4) involve the difference in kinetic, exchange, and correlation energies in going from the case of isolated atoms to the solid. The last term is the electrostatic energy of the overlapping charge distributions.

Consider the region around atom i. Let us define the background density for atom i to be $\rho_{b,i}(r)\equiv\sum_{j\,(\neq i)}\rho_j^a(r-R_j)$. In most of this region, the density ρ_i^a dominates in ρ_s; $\rho_{b,i}(r)$ is small and slowly varying compared to ρ_i^a. Thus it seems plausible to approximate $\rho_{b,i}$ by a constant $\bar\rho_i$. (The best value of $\bar\rho_i$ will be determined later in this section.) Let us therefore define the embedding energy for an atom in an electron gas of some constant density $\bar\rho$ (neutralized by a positive background):

$$G_i(\bar\rho_i)\equiv G[\rho_i^a+\bar\rho_i]-G[\rho_i^a]-G[\bar\rho_i]\ . \tag{5}$$

Using the embedding energy, we can rewrite the cohesive energy as

$$E_{\rm coh}=\sum_i G_i(\bar\rho_i)+\tfrac{1}{2}\sum_{ij}U_{ij}^a+E_{\rm err}\ , \tag{6}$$

where the error is

$$E_{\rm err}=G\left[\sum_i\rho_i^a\right]-\sum_i G[\rho_i^a+\bar\rho_i]+\sum_i G[\bar\rho_i]=\int_\infty\left[g\left[\sum_i\rho_i^a\right]-\sum_i g(\rho_i^a+\bar\rho_i)+\sum_i g(\bar\rho_i)\right]\ . \tag{7}$$

Setting $E_{\rm err}=0$ provides a definition for the optimal background densities $\bar\rho_i$. For a homogeneous, homonuclear solid, each atom experiences the same environment, so that $\bar\rho_i=\bar\rho$ for all i. However, for inhomogeneous environments, we need an equation for each $\bar\rho_i$. This is provided by breaking up the integral in Eq. (7) into integrals over the region around each atom i,

$$\sum_i\left[\int_{\Omega_i}[g(\rho_i^a+\rho_{b,i})-g(\rho_i^a+\bar\rho_i)+g(\bar\rho_i)]-\int_{\infty-\Omega_i}[g(\rho_i^a+\bar\rho_i)-g(\bar\rho_i)]\right]=0\ , \tag{8}$$

where the region around atom i is Ω_i and $\infty-\Omega_i$ is the remainder. In practice, the solution to Eq. (8) is not very sensitive to the choice of Ω_i. Here we require that each term in the summation vanish independently, giving a separate condition for each $\bar\rho_i$ which depends on the environment local to atom i. The solution of this equation is discussion in Sec. II C. For now we will note that $\bar\rho_i$ is a functional of $\rho_{b,i}$:

$$\bar\rho_i=\bar\rho_i[\rho_{b,i}]\ , \tag{9}$$

where the functional depends on the nature of g and ρ_i^a.

Equations (5), (6), and (9) now provide a relationship between the embedding energy and the cohesive energy. The difference between these equations and Eq. (3) is that the evaluation of the functional $G[\rho]$ for the solid is reduced to evaluating the embedding function $G(\bar\rho_i)$ for each atom. This is an advantage only if the functional in Eq. (9) can be approximated in a relatively simple way. In that case, atomistic calculations become very straightforward.

B. Effect of charge relation

The effect of charge redistributions can be absorbed into equations of the same form as Eqs. (5), (6), and (9), provided the redistributions are small enough to be treated in lowest order. To demonstrate this, let us denote the

redistribution by $\Delta(r)$. Substituting $\rho(r)=\rho_s(r)+\Delta(r)$ into Eq. (3) gives

$$E_{\rm coh}=G\left[\sum_i \rho_i^a+\Delta(r)\right]-\sum_i G[\rho_i^a] +\tfrac{1}{2}\sum_{ij}{}' U_{ij}^a+\int d\mathbf{r}\, V_s(r)\Delta(r) +\tfrac{1}{2}\int d\mathbf{r}_1\int d\mathbf{r}_2\frac{\Delta(r_1)\Delta(r_2)}{r_{12}}\ , \tag{10}$$

with

$$V_s(r)\equiv\sum_i V_i^a(r)\ ,$$

and

$$V_i^a(r)\equiv\frac{-Z_i}{r}+\int d\mathbf{r}\frac{\rho_i^a(r'-R_i)}{|r-r'|}$$

is the Hartree potential of atom i.

For a homogeneous crystal the equation for Δ is (to first order in Δ)

$$g'(\rho_s(r))+\int d\mathbf{r}' g''(\rho_s(r),\rho_s(r'))\Delta(r') +V_s(r)+\int d\mathbf{r}'\frac{\Delta(r')}{|r-r'|}=\mu\ , \tag{11}$$

where Δ depends on the chemical potential μ, which is determined by requiring that $\int_{\Omega_i}\Delta(r)d\mathbf{r}=0$. Here we have denoted

$$g'(\rho(r))\equiv\frac{\delta}{\delta\rho(r)}G[\rho]=\left[\frac{\partial}{\partial\rho}-\nabla\cdot\frac{\partial}{\partial\nabla\rho}+\nabla^2\frac{\partial}{\partial\nabla^2\rho}-\cdots\right]\gamma(\rho(r),\nabla\rho(r),\nabla^2\rho(r),\ldots)\ , \tag{12a}$$

$$g''(\rho(r),\rho(r'))\equiv\frac{\delta^2}{\delta\rho(r)\delta\rho(r')}G[\rho]=\delta(r-r')\left[\frac{\partial^2\gamma}{\partial\rho^2}-2\nabla\cdot\left[\frac{\partial^2\gamma}{\partial\nabla\rho\,\partial\rho}\right]\right]\Bigg|_\sigma+\nabla_{\mathbf{r}}\nabla_{\mathbf{r}'}:\left[\delta(r-r')\frac{\partial^2\gamma}{\partial\nabla\rho^2}\Bigg|_\sigma\right]+\cdots\ , \tag{12b}$$

with $\sigma=(r+r')/2$.

Consider again the region around atom i. As before, we note that in most of this region $\rho_{b,i}(r)$ is small and slowly varying compared to $\rho_i^a(r)$, so it seems plausible to approximate this by a constant $\bar\rho_i$. That is, we take $\rho_s(r)=[\rho_i^a(r)+\bar\rho_i]+[\rho_{b,i}(r)-\bar\rho_i]$ and treat the second group as a perturbation on the first. We also treat V_s perturbatively: $V_s(r)=V_i^a(r)+V_{b,i}(r)$, where $V_{b,i}(r)\equiv\sum_{j\,(\neq i)}V_j^a(r-R_j)$ is the contribution to the Hartree potential in region i from the neighbors of atom i. [We could have introduced a $\bar V_i$, analogous to $\bar\rho_i$, but a constant background potential has no effect on the charge redistribution. So, in fact, the perturbation on the potential is the *nonuniformity* of $V_{b,i}(r)$ rather than its magnitude.] Carrying out a perturbation in $\rho_{b,i}-\bar\rho_i$ and $V_{b,i}$ changes Eq. (11) to

$$g'(\rho_i^a+\bar\rho_i)+\int d\mathbf{r}'\, g''(\rho_i^a+\bar\rho_i)\Delta(r')+V_i^a+\int d\mathbf{r}'\frac{\Delta(r')}{|r-r'|} +\left[\int g''(\rho_i^a+\bar\rho_i)[\rho_{b,i}^a(r')-\bar\rho_i]+V_{b,i}\right]=\mu\ . \tag{13}$$

The lowest order form of this equation (neglecting the terms in large parentheses),

$$g'(\rho_i^a+\bar\rho_i)+\int d\mathbf{r}'\, g''(\rho_i^a+\bar\rho_i)\Delta_i(r')+V_i^a +\int d\mathbf{r}'\frac{\Delta_i(r')}{|r-r'|}=\mu\ , \tag{14}$$

describes the electronic redistribution around an atom in a constant background electron gas of density $\bar\rho_i$. The solution to Eq. (14) (Δ_i) differs from the solution to Eq. (13) (Δ) only to first order in $\rho_{b,i}-\bar\rho_i$ and $V_{b,i}$ [these are the terms in large parentheses in Eq. (13)]. Therefore, in the region dominated by atom i, $\Delta\approx\Delta_i+O((\rho_{b,i}-\bar\rho_i),V_{b,i})$. This suggests approximating $\Delta(r)$ by $\Delta_s(r)\equiv[\sum_i\Delta_i(r-R_i)]$. The error is expected to be the largest in the bonding region between the atoms.

The error in the cohesive energy caused by replacing Δ by Δ_s is

$$\tfrac{1}{2}\int d\mathbf{r}\int d\mathbf{r}'\left[g''(\rho_s(r),\rho_s(r'))+\frac{1}{|r-r'|}\right] \times[\Delta(r)-\Delta_s(r)][\Delta(r')-\Delta_s(r')]\ .$$

This error is second order in the *error in the electron redistribution,* and we have assumed that the redistribution itself is small. In the region dominated by an atom, the error is smallest. The largest contribution to the error comes from the bonding region between atoms, where the superposition has the largest error. This echoes the previous statement that the EAM approximation is not expected to work well where covalent bonding is strong.

Rewriting Eq. (10) using Δ_s in place of Δ gives

$$E_{\rm coh}=G\left[\sum_i(\rho_i^a+\Delta_i)\right]-\sum_i G[\rho_i^a]+\tfrac{1}{2}\sum_{i,j}{}' U_{ij}^a +\sum_{i,j}\int d\mathbf{r}\, V_i^a(r)\Delta_j(r) +\tfrac{1}{2}\sum_{i,j}\int d\mathbf{r}_1\int d\mathbf{r}_2\frac{\Delta_i(r_1)\Delta_j(r_2)}{r_{12}}\ . \tag{15}$$

From here the argument proceeds as before. We define an embedding energy allowing for charge relaxation:

$$G_i(\bar\rho_i^{\,*})\equiv G[\rho_i^a+\Delta_i+\bar\rho_i^{\,*}]-G[\rho_i^a] -G[\bar\rho_i^{\,*}]+\int d\mathbf{r}\, V_i^a(r)\Delta_i(r) +\tfrac{1}{2}\int d\mathbf{r}\int d\mathbf{r}'\frac{\Delta_i(r')\Delta_i(r)}{|r-r'|}\ . \tag{16}$$

[The embedding energy in Eq. (16) is indeed minimized by the charge redistribution Δ_i because of Eq. (14).] We can rewrite the cohesive energy as

$$E_{\rm coh}=\sum_i G_i(\bar\rho_i^*)+\tfrac{1}{2}\sum_{i,j}U_{ij}\ , \tag{17}$$

where U_{ij} is defined similarly to U_{ij}^a [following Eq. (4)], but with $\rho^a+\Delta$ replacing ρ^a. Equation (17) is valid, provided that the error

$$E_{\rm err}=\int_\infty \left[g\left[\sum_i(\rho_i^a+\Delta_i)\right]-\sum_i g(\rho_i^a+\bar\rho_i^*+\Delta_i)+\sum_i g(\bar\rho_i^*)\right] \tag{18}$$

vanishes. This is the same as Eq. (7) with $\rho_i^a+\Delta_i$ replacing ρ_i^a, so that the solution is

$$\bar\rho_i^*=\bar\rho_i^*[\rho_{b,i}+\Delta_{b,i}]\ , \tag{19}$$

where $\Delta_{b,i}$ is defined analogous to $\rho_{b,i}$ and the functional $\bar\rho_i^*$ is different from $\bar\rho_i$ because of Δ_i.

Using Eq. (17) involves solving Eqs. (14) and (19) iteratively, and also U_{ij} depends on Δ. However, the charge redistribution Δ is relatively independent of ρ (Ref. 26), so that the modification due to electronic relaxations does not really change the qualitative form of the EAM expression. Therefore, charge redistribution would be absorbed quite naturally in an empirical determination of the EAM functions, provided that the charge relaxations are small.

C. Determination of the optimum background density

We turn now to the problem of solving Eq. (8). [The solution to Eq. (18), which allows first-order charge redistribution, is analogous.] In general, there is no simple solution to this equation. We will discuss in this section various approximations to the solution, and in Sec. III we will solve this equation numerically for a specific model function g.

Because ρ_i^a decays exponentially, the integral in the region outside of Ω_i is of secondary magnitude and a good solution to Eq. (8) is provided by neglecting the contribution from $\infty-\Omega_i$. Thus let us examine

$$\int_{\Omega_i}[g(\rho_i^a+\rho_{b,i})-g(\rho_i^a+\bar\rho_i)+g(\bar\rho_i)]=0 \tag{20}$$

to get an idea of the nature of the solution.

The kinetic-energy part of g dominates the integrand in Eq. (20). Near the nucleus of atom i, the kinetic energy is largely due to the orthogonalization of the valence states to the core states. In the statistical Thomas-Fermi model, $g(\rho)\sim\rho^{5/3}$. Kress and DePristo[24] suggest approximating $g(\rho)\sim\rho^{5/3}$ by $c_1\rho+c_2\rho^2$. Substituting this into Eq. (20) gives

$$\bar\rho_i=\left[c_1\int d\mathbf{r}\,\rho_{b,i}(r)+2c_2\int d\mathbf{r}\,\rho_i^a\rho_{b,i}(r)+c_2\int d\mathbf{r}\,[\rho_{b,i}(r)]^2\right]\left[2c_2\int d\mathbf{r}\,\rho_i^a(r)\right]^{-1}.$$

If we neglect the first and last terms in the large parentheses compared to the second, then we get the approximate solution of Kress and DePristo: $\bar\rho_i=\int d\mathbf{r}\,w_i(r)\rho_{b,i}(r)$ with $w_i(r)=\rho_i^a[\int d\mathbf{r}\,\rho_i^a(r)]^{-1}$ playing the role of a linear weighting function.

Previous approaches have used various linear weighting functions. Nørskov[20] originally argued that $\bar\rho$ should be determined by weighting the $\rho_{b,i}$ by the Hartree potential of the atom: $w_i(r)=V_{h,i}(r)[\int d\mathbf{r}\,V_{h,i}(r)]^{-1}$. Jacobsen *et al.*[22] proposed to simply average the background density over the cell, so that $w_i(r)=1/\Omega_i$ for $\mathbf{r}\in\Omega_i$ and 0 for $\mathbf{r}\notin\Omega_i$. The extreme in localization, of course, would be $w_i(r)=\delta(r-R_i)$.

However, in fact, no linear weighting function solves Eq. (20) in general. In the region between atoms, near the edge of Ω_i, the kinetic energy is largely due to the few interstitial electrons, so that the form of $g(\rho)$ is more like $|\nabla\rho|^2/\rho$. To the extent that this term is non-negligible, the optimum $\bar\rho$ cannot be obtained by a weighted integral over the background density.

This is made clearer by examining the functional derivative of $\bar\rho$:

$$w_i(r)\equiv\frac{\delta\bar\rho}{\delta\rho_b(r)}=g'(\rho_i^a(r)+\rho_b(r))\times\left[\int_{\Omega_i}[g'(\rho_i^a(r)+\bar\rho)-g'(\bar\rho)]\right]^{-1}.$$

In the limit of both $\bar\rho_i$ and $\rho_{b,i}(r)\ll\rho_i^a$, we find that

$$w_i(r)=g'(\rho_i^a(r))\left[\int_{\Omega_i}g'(\rho_i^a(r))d\mathbf{r}\right]^{-1}. \tag{21}$$

This weighting function is largely determined by the orthogonalization to the core states near the nucleus, and is therefore largely localized. The use of a localized weighting function is approximately justified. But, in general, the background density is not small compared to the density of the central atom on the edge of Ω_i, so that the weighting function solution to Eq. (20) has some error.

Another way of examining the solution to Eq. (20), which is equivalent, is to assume that the background density is largely constant with small variations. That is, we approximate the background density

$$\rho_b(r)+\Delta_b(r)\equiv\tilde\rho(r)\approx\tilde\rho(0)+\mathbf{r}\cdot\nabla\tilde\rho(0)+\tfrac{1}{2}\mathbf{rr}:\nabla\nabla\tilde\rho(0)\ ,$$

and expand in a Taylor's series involving powers of $\nabla\tilde\rho(0)$ and $\nabla\nabla\tilde\rho(0)$. We find that the gradient term does not contribute to first order, leaving

$$\bar\rho=\tilde\rho(0)+\alpha\nabla^2\tilde\rho(0)\ , \tag{22}$$

with

$$\alpha\equiv\int_{\Omega_i}\left[\frac{\partial\gamma}{\partial\rho}+2\mathbf{r}\cdot\frac{\partial\gamma}{\partial\nabla\rho}\right]\left[6\int_{\Omega_i}\left[\frac{\partial\gamma}{\partial\rho}\right]\right]^{-1}.$$

Higher-order corrections can be made similarly. To second order,

$$\bar\rho=\tilde\rho(0)+\alpha'\nabla^2\tilde\rho(0)+\beta|\nabla\tilde\rho(0)|^2\ . \tag{23}$$

Again, these relations are only approximate, due to the breakdown in the Taylor's-series expansion near the edge of Ω_i.

Thus the trend is for $\bar\rho$ to reflect the profile of the back-

ground density nearest the nucleus, but the profile of the background density further away is not completely negligible. In practice, however, the density over the whole Ω is *related* to the density tails at the nucleus, so that in fact $\bar{\rho}$ may be closely related to the density profile near the nucleus, even though the strict solution to Eq. (20) does not make this apparent. This is demonstrated in Sec. III, where we obtain the numerical solution for $\bar{\rho}$ for a model g involving both the Thomas-Fermi and gradient terms. The exact solution will be examined in terms of the simple approximations suggested here. Indeed, in that case, there is a simple relation between $\bar{\rho}$ and the density at the origin, which is approximately given by Eq. (22).

In the usual implementation of the EAM, there is assumed a unique relationship between the $\bar{\rho}$ and the background density at the origin. Obviously this is true for the extremely localized case of $w_i(r)=\delta(r-R_i)$. However, it may also be a reasonable approximation even for more complicated solutions. In that case, we simply require that the density at the origin be a reasonable monitor of $\bar{\rho}$.

D. An alternate definition

In this subsection we will describe an alternate grouping of terms in the total energy. Some of the interactions contained in U_{ij} may be grouped with the embedding function and the derivation carried through as before. It is important to note that though the resulting embedding function and pair interaction are different than before, the resulting total energy is unchanged. The motivation for the alternate grouping is purely for practical reasons, which will be discussed.

The functions in Eq. (6) differ somewhat from those frequently used in practical implementations of Eq. (1). As defined in Eq. (5), $G(\bar{\rho})$ represents the embedding energy of an atom in a *neutral* electron gas (jellium), and should be compared to calculations of an atom in jellium. The explicitly electrostatic interactions occurring in the solid are contained in U. An alternate way of partitioning the cohesive energy is to define an embedding energy in an electron gas without the uniform positive background, as is the case in a solid. In this case, the electrostatic interaction of the background electron gas with the Hartree potential of the atoms should be included in the embedding energy. In this view, an alternate embedding function is

$$F_i(\bar{\rho})\equiv G_i(\bar{\rho})+\bar{\rho}\,\bar{V}_i^a\ , \tag{24}$$

where the average Hartree potential is $\bar{V}_i^a\equiv\int V_i^a$. This view changes none of the arguments, but simply includes some of the electrostatic interactions in the definition of an alternate embedding function.

The cohesive energy in terms of F is

$$E_{\rm coh}=\sum_i F_i(\bar{\rho}_i)+\tfrac{1}{2}\sum_{ij}\phi_{ij}^a\ , \tag{25}$$

where the pair interaction

$$\phi_{ij}^a\equiv\frac{Z_iZ_j}{R_{ij}}-\int d\mathbf{r}_1\int d\mathbf{r}_2\frac{\rho_i^a(r_1)\rho_j^a(r_2)}{r_{12}} \tag{26}$$

is positive definite.

The calculation of the error is very similar. The background density is done in an analogous way, and for the linear case the weighting function is modified to

$$w_i(r)=\{g'(\rho_i^a(r))+V_i^a(r)\}\times\left[\int_{\Omega_i}\{g'(\rho_i^a(r))+V_i^a(r)\}\right]^{-1}\ . \tag{27}$$

The weighting function is still very localized to the nucleus, because of the nature of the Hartree potential. Of course, the same *caveat* applies to this weighting function that was discussed in Sec. II C.

There is, in effect, no distinction between the two ways of defining the embedding function. For practical reasons, the (F,ϕ) set [Eqs. (25) and (26)] has been used most often in the past.[7,10] In some work, the authors assumed that the pair interaction between two different types of atoms obeyed a geometric mean: $\phi_{ij}(R)=[\phi_{ii}(R)\phi_{jj}(R)]^{1/2}$, which, of course, required a positive-definite function. This restriction was placed on the functions *solely to reduce the number of free parameters* during the semiempirical fitting. For two similar elements, the error is reasonable.[27] Actually, a somewhat better approximation is an arithmetic mean: $\phi_{ij}(R)=\frac{1}{2}[\phi_{ii}(R)+\phi_{jj}(R)]$, which could be applied as well to the (G,U) set. Therefore the traditional, practical reason for choosing the (F,ϕ) picture is not really a concern.

There should be no confusion caused by two different sets of embedding function and pair potential. In fact, the transformation $G(\rho)\rightarrow G(\rho)+2c\rho$ and $U(R)\rightarrow U(R)-c\rho^a(R)$ for arbitrary c leaves the total energy unchanged. Therefore, two different looking sets of functions may, in fact, be very similar in their total energy. The relationship between the (F,ϕ) set and the (G,U) set is simply an example of this transformation. We discuss ways to compare different sets in Sec. III.

E. Summary of derivation

In summary, the cohesive energy can be written

$$E_{\rm coh}=\sum_i G_i(\bar{\rho}_i)+\tfrac{1}{2}\sum_{i,j}U_{ij}^a\ ,$$

where U contains the two-body electrostatic interactions and the embedding function is given by

$$G_i(\bar{\rho}_i)\equiv G[\rho_i^a+\bar{\rho}_i]-G[\rho_i^a]-G[\bar{\rho}_i]\ .$$

The constant background density is given by solving

$$\int_{\Omega_i}[g(\rho_i^a+\rho_{b,i})-g(\rho_i^a+\bar{\rho}_i)+g(\bar{\rho}_i)]=0$$

for each atom. In general, a fairly good approximation for $\bar{\rho}_i$ is given by a weighted integral of $\rho_{b,i}$, with the weighting function given by

$$w_i(r)=g'(\rho_i^a(r))\left[\int_{\Omega_i}d\mathbf{r}\,g'(\rho_i^a(r))\right]^{-1}\ ,$$

which is localized to the nucleus. This derivation is based on the assumption that the charge distribution in the solid is not very different from a superposition of

atomic electron densities; thus this form is restricted to simple metals and early or late transition metals.

We will demonstrate the procedure outlined in this section by testing the approximations on a model system. In particular, we will set up a model quantum mechanics which describes fcc nickel quite well, and where the approximations assumed in this section are expected to be valid. In particular, the equation for the optimum electron density is solved in detail and a simple relationship is found between $\bar{\rho}$ and the background density at the origin. Thus the EAM form is heuristically justified.

III. MODEL SYSTEM

To examine the arguments in the preceding section more carefully, we will develop a simple model of fcc nickel. We will neglect in this calculation the charge redistributions, calculating instead the electron charge density from the superposition of atomic densities. We will calculate the cohesive energy from Eq. (4) and demonstrate that the model also represents various simple defect energies of fcc nickel very well. We will then show that Eq. (4) is represented well by Eq. (6). We will examine the embedding energy and electrostatic interaction. We will also examine the solution for the optimum constant background density and show that it is related in a simple way to the background density at the origin.

For this section, we will use the local-density functional for the energy, using local exchange and correlation, and the Thomas–Fermi–Dirac–von Weizsäcker (TFDvW) functional for the kinetic energy. A similar energy functional combined with a pseudopotential gave very reasonable values for cohesive energies and lattice constants for the alkali metals.[28] Here we will use the full potential and charge density, with the assertion that the TFDvW functional should work well also in the case for Ni, which has an almost filled d shell. Explicitly, for this calculation we take the kinetic-exchange-correlation-energy density to be[29]

$$g(\rho)=t(\rho)+x(\rho)+c(\rho)\ , \tag{28a}$$

with the exchange-energy density

$$x(\rho)=-\frac{3}{4}\left[\frac{3}{\pi}\right]^{1/3}\rho^{4/3} \tag{28b}$$

and the correlation-energy density

$$c(\rho)=\rho\left[-0.0575+0.0155\ln\left[\frac{3}{4\pi\rho}\right]^{1/3}\right]. \tag{28c}$$

The kinetic-energy density is based on the von Weizsäcker gradient correction[30] to the Thomas-Fermi term:

$$t(\rho)=\frac{3}{10}\left[\frac{3}{\pi^2}\right]^{2/3}\rho^{5/3}+\frac{\lambda}{8}\frac{|\nabla\rho|^2}{\rho}\ . \tag{28d}$$

Perturbations around a uniform electron gas have a kinetic energy density of the form in Eq. (28d) in two limits: $\lambda=1$ for rapidly varying perturbations[31] and $\lambda=\frac{1}{9}$ for slowly varying perturbations.[32] We will consider λ to be adjustable in this work.

In calculating the cohesive energy of fcc nickel from Eq. (4), one needs to specify the atomic density (i.e., the atomic configuration) and the parameter λ. In this work, we modify the $3d^8 4s^2$ atomic density[33] for Ni by scaling the $3d$ and $4s$ densities linearly according to a parameter n_s: $\rho_{\rm Ni}(r)=\rho_{\rm core}(r)+n_s\rho_{4s}(r)+(10-n_s)\rho_{3d}(r)$. We then adjust λ and n_s to match the predicted equilibrium lattice constant and cohesive energy to the experimental values.[34,35] This gives $\lambda=0.384$ and $n_s=1.33$. Both of these parameters are within their physically reasonable ranges. (Also, λ is close to the value of 0.48 used in Ref. 28.) The following calculations use these values.

Equation (4) is solved numerically in the following way. The kinetic, exchange, and correlation functionals were integrated by a three-dimensional quadrature in the appropriate cell. For the bulk cohesive energy, for example, 44 000 points were required in the irreducible Wigner-Seitz cell to get good convergence. The calculations of the vacancy formation energy and surface energies required over 2×10^6 points, because of reduced symmetry. Also, for the vacancy and surface calculations, the energy of atoms out to third neighbor were sufficiently different from the value in bulk that these changes had to be calculated. The electrostatic interactions were calculated seminumerically by first taking the Fourier transform of the Clementi functions and doing most of the integration analytically.

In Fig. 1 we show the cohesive energy of fcc nickel as a function of lattice constant. (Recall that λ and n_s were adjusted to match the lattice constant and cohesive energy to the experimental values of 6.64 bohrs and -0.164 hartree.) For comparison, Moruzzi *et al.*[36] calculate from the local-density approximation a lattice constant of 6.55 bohrs and cohesive energy of -0.206 hartree.

To test the reliability of the model proposed for nickel, we have calculated the energy in Eq. (4) for a variety of

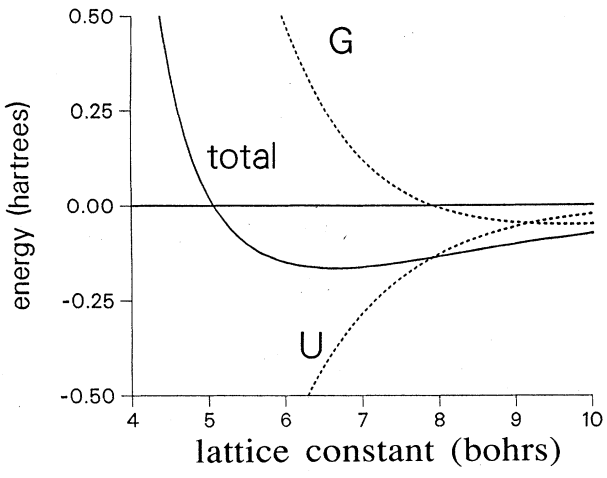

FIG. 1. The cohesive energy of fcc nickel as a function of lattice constant, calculated in the manner described in the text. The contributions identified as kinetic energy, exchange and correlation energies (G), and electrostatic energy (U) are shown as dotted curves.

situations where experimental data are available. These quantities are presented in Table I. The first two entries (fcc lattice constant and cohesive energy) were fitted to experiment. The remaining are predictions. The agreement with available experimental data is quite good. Note, in particular, that the surface energies are in good agreement with the value obtained experimentally for an "average" surface, and that the (111) surface is the most stable, as should be. The energies of the bcc and hcp phases are very slightly more positive than the fcc phase; they are quoted as +0.00 to indicate that, to within the accuracy of the numerical quadrature, the energy differences are essentially zero.

Also from the quantities in Table I, it is evident that the TFDvW functional gives a good description of the many-body character of the interatomic interactions. A purely two-body interaction yields a vacancy-formation energy equal to the cohesive energy, whereas experimentally the vacancy-formation energy is about $\frac{1}{3}$ of the cohesive energy. Similarly, the surface energy in a strictly two-body interaction is much higher than is experimentally observed. The many-body corrections in the EAM, which have been discussed in detail elsewhere,[9,16] come from the nonlinearity of the embedding function (principally, the nonlinearity of the kinetic energy).

Given a reasonable model of defects and surfaces in Ni, we will now use that model to calculate the corresponding EAM forms described in Sec. II.

The embedding function $G_{\mathrm{Ni}}(\bar{\rho})$ is calculated from Eq. (5). This is done numerically, but the quadrature here is reduced to one dimension by symmetry. The result is plotted in Fig. 2. The embedding function has the desired behavior: simple minimum at lower densities and nearly linear upward slope at higher densities.

TABLE I. Values of quantities calculated using the TFDvW method (see text), compared to experiment where available, and also compared to the first-principles EAM (FP-EAM) calculations using functions based on approximations to the TFDvW method.

Quantity	TFDvW	Experiment	FP-EAM
fcc lattice constant (bohrs)	6.64	6.64[a]	6.61
Cohesive energy (hartree)	0.164	0.164[b]	0.163
Bulk modulus (Mbar)	1.2	1.8[c]	1.4
Elastic constants (10^{12} ergs/cm^2)			
C_{11}		2.465[c]	1.544
C_{12}		1.473[c]	1.307
C_{44}		1.247[c]	0.602
Vacancy formation (eV)	1.4	1.6[d]	1.4
Vacancy volume (Ω_0)			−0.38
Divacancy binding (eV)		0.33[e]	0.12
Surface energies (ergs/cm^2)			
(100)	2398		1682
(110)	2585	2380[f]	1810
(111)	2305		1571
Surface relaxations (Å)			
(100)			
Δz_{12}		0.00[g]	−0.03
Δz_{23}			−0.02
(110)			
Δz_{12}		−0.06 to −0.10[g]	−0.09
Δz_{23}			+0.01
Δz_{34}			−0.01
(111)			
Δz_{12}		−0.025 to 0.0[g]	−0.03
Δz_{23}			−0.002
bcc-fcc energy difference (hartree)	+0.00	+0.002[h]	+0.00
bcc lattice constant (bohrs)	5.25		5.26
hcp-fcc energy difference (hartree)	+0.00	+0.0004[h]	+0.00

[a]Reference 34.
[b]Reference 35.
[c]Reference 37.
[d]Reference 38.
[e]Reference 39.
[f]Reference 40 (Value is estimated from liquid-solid–interface energy and represents an average of surface orientations.)
[g]Summary of data detailed in Ref. 7 and references therein. Experimental errors are generally quoted as ±0.02 Å.
[h]Reference 41.

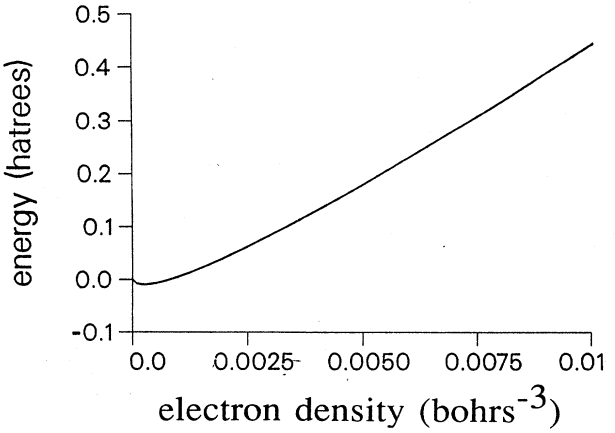

FIG. 2. The embedding energy for nickel as a function of the background electron density, calculated in the manner described in the text.

The electrostatic interaction, $U_{\text{Ni-Ni}}(R)$, is calculated and shown in Fig. 3.

The embedding and electrostatic energies (Figs. 2 and 3) sum to the total energy (Fig. 1), provided the $\bar{\rho}$ satisfies $E_{\text{err}}(\bar{\rho})=0$. For the case of the homogeneous environments (fcc, bcc, and hcp), we note that all $\bar{\rho}_i=\bar{\rho}$, and divide the solid into equal Wigner-Seitz cells Ω. We then evaluate

$$\int_{\Omega_i}\left[g\left[\rho_i^a+\sum_{j(\neq i)}\rho_j^a\right]-g(\rho_i^a+\bar{\rho})+g(\bar{\rho})-\sum_{j(\neq i)}g(\rho_j^a+\bar{\rho})+\sum_{j(\neq i)}g(\bar{\rho})\right]$$

numerically by three-dimensional quadrature and search for a zero in the function. For the inhomogeneous environments, such as a surface, the value of $\bar{\rho}_i$ will depend on the distance from the defect. Here we assume that $\bar{\rho}_i=\bar{\rho}_{\text{surf}}$ for atoms which are on the surface and $\bar{\rho}_i=\bar{\rho}_{\text{bulk}}$ for all other atoms. This is reasonable, in that the second-neighbor contribution to $\bar{\rho}$ is much less than that for the first neighbor. In that case, we evaluate for an atom i on the surface:

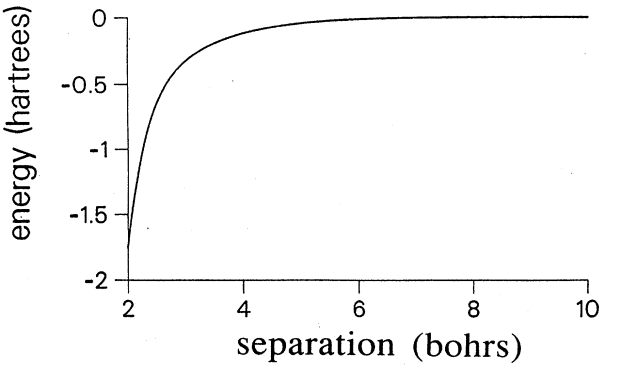

FIG. 3. The electrostatic interaction between nickel atoms as a function of separation.

$$\int_{\Omega_i}\left[g\left[\rho_i^a+\sum_{j(\neq i)}\rho_j^a\right]-g(\rho_i^a+\bar{\rho}_{\text{surf}})+g(\bar{\rho}_{\text{surf}})-\sum_{j(\neq i)}g(\rho_j^a+\bar{\rho}_j)+\sum_{j(\neq i)}g(\bar{\rho}_j)\right],$$

where $\bar{\rho}_j=\bar{\rho}_{\text{surf}}$ for j on the surface and $\bar{\rho}_j=\bar{\rho}_{\text{bulk}}$ for j otherwise. We then find a $\bar{\rho}_{\text{surf}}$ which makes this function zero. We have thus found $\bar{\rho}$ for the following environments: fcc and bcc lattices at several lattice constants and the (100), (110), and (111) surfaces of fcc lattices.

Anticipating that the dependence of $\bar{\rho}$ on the background density is mostly localized, we have plotted in Fig. 4 the values of $\bar{\rho}$ for these various environments versus the background density at the nucleus. There is a reasonable correlation between $\bar{\rho}_i$ and $\rho_{b,i}(R_i)$, for a surprising range of environments. Most notably, the $\bar{\rho}$ is very similar for fcc and bcc lattices with the same density at the nucleus, and also for surface atoms. Fitting a linear function through the points near the equilibrium for the fcc lattice gives $\bar{\rho}_i=0.96\rho_{b,i}(R_i)-7.443\times10^{-4}/\text{bohr}^3$, and this line is plotted on Fig. 4. The deviation from this fitted line is small for all points, largest for the surfaces.

The linear relationship can be mostly understood in terms of the localization of a linear weighting function. To emphasize the localized nature of the solution to $E_{\text{err}}=0$, we have plotted in Fig. 5 the linear weighting function from Eq. (21) and the background density for the case of bulk fcc nickel at equilibrium. Figure 5 demonstrates that the weighting function is most sensitive to the background density near the nucleus. We can estimate from Eq. (22) the first-order correction due to the nonuniformity of the background density, and this gives $\bar{\rho}_i=0.95\rho_{b,i}(R_i)$, which has about the right slope as compared to Fig. 4.

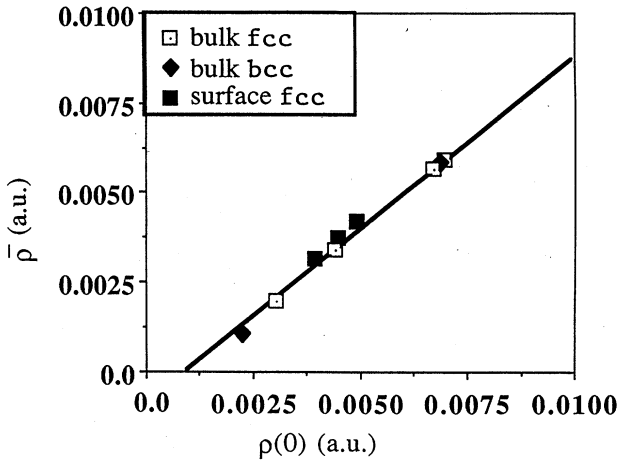

FIG. 4. The optimal background density ($\bar{\rho}$) vs the background density at the nucleus [$\rho_b(0)$] from a linear superposition, for various atomic environments. The $\rho_b(0)$ for fcc lattice at equilibrium is 6.7×10^{-3} a.u.; for the bcc lattice at equilibrium, it is 6.9×10^{-3} a.u. There are several points at higher densities not shown on this plot, which show that the linear relationship holds beyond $\rho_b(0)=0.05$.

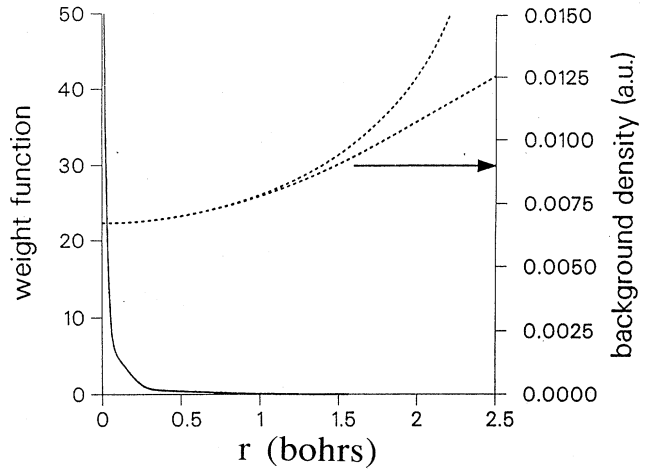

FIG. 5. The effective weighting function from Eq. (21) for a nickel atom, and the background density in a nickel lattice site as a function of distance from the nucleus. The two lines for the background density represent the range of values spanned by the variation with angle.

There are some deviations of $\bar{\rho}$ from an exact relationship with the background density, most notably the surfaces compared to the expanded lattice. These deviations indicate that the concept of a linear weighting function solution is only approximate, as discussed in Sec. II. Also, the nonzero offset is inconsistent with the simple weighting function solution, and is a result of the nonlinear nature of Eq. (20). However, we can make use of the approximate relationship between $\bar{\rho}$ and the background density at the origin. All we need to make use of Eq. (4) is a relationship between $\bar{\rho}$ for atom i and the positions of its neighbors. This is provided to a good approximation by the linear fit shown in Fig. 4. In the following, we use this linear fit, noting that the error in the fit is largest for the surface.

We therefore have constructed EAM functions, obtained from nearly first principles, to describe Ni. Predictions of defect properties using these EAM functions are presented in Table I. Most of the properties are represented rather well, the worst being the elastic constants. The surface energies in the EAM differ from the TFDvW values because the linear relationship between $\bar{\rho}_i$ and $\rho_{b,i}(R_i)$ is worst for the surface. The small deviations in Fig. 4 between the correct values for $\bar{\rho}_i$ at the surface and the linear relationship are responsible for the discrepancy between the surface energies calculated in the TFDvW functional and the EAM. A better form, such as $\bar{\rho}=\tilde{\rho}(0)+\alpha\nabla^2\tilde{\rho}(0)+\beta|\nabla\tilde{\rho}(0)|^2$, probably better represents the $\bar{\rho}$ in most environments.

The values of the calculated properties shown in Table I are quite a bit off when compared to the values that can be obtained semiemprically. It seems interesting therefore to compare the functions to the semiempirical functions which are fitted to such properties as the elastic constants, etc. Because of the linear transformations discussed in Sec. II D, a direct comparison of embedding functions, etc. is not physically meaningful. Rather, a measure of the energetics of defects can best be obtained by calculating changes in the total energy due to distortions in the system. For small distortions, the change in the energy within the EAM is equivalent to the change in the sum of effective two- and three-body interactions:[9]

$$\varphi_{ij}(R)\equiv\tfrac{1}{2}(\{U_{ij}(R)+2G_i'(\bar{\rho}_i)\rho_j^a(R)+G_i''(\bar{\rho}_i)[\rho_j^a(R)]^2\}+(i\leftrightarrow j))\ , \tag{29a}$$

$$\chi_{ijk}(R_i,R_j,R_k)\equiv[G_i''(\bar{\rho}_i)\rho_j^a(R_{ij})\rho_k^a(R_{ik})+\text{c.p.}]\ . \tag{29b}$$

Note that these interactions are independent of the transformation discussed in Sec. II D, and represent quantities which can be directly compared between different sets of

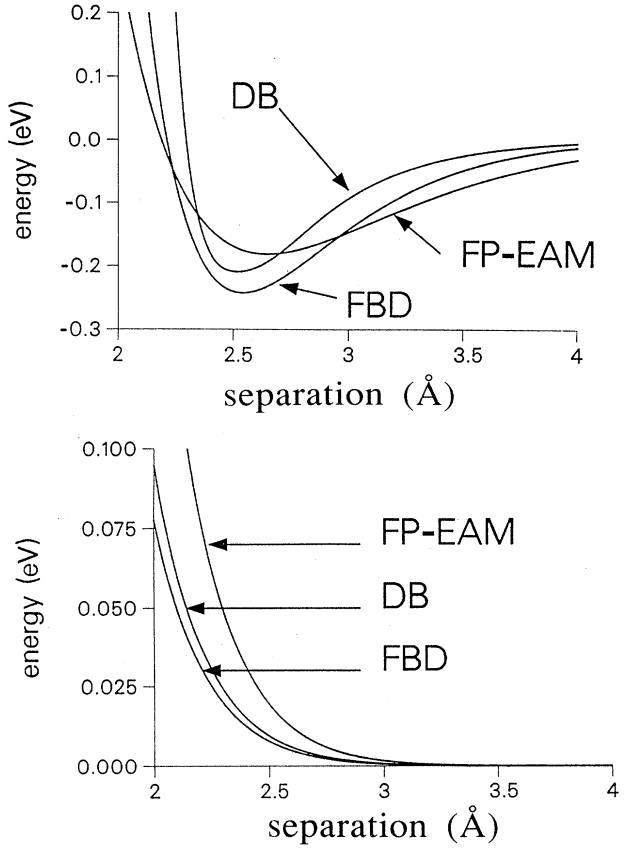

FIG. 6. Effective interactions for three EAM functions for nickel. "DB" are the Daw-Baskes EAM functions from Ref. 7 and were fitted to the lattice constant, elastic constants, sublimation energy, vacancy-formation energy, and bcc-fcc phase stability. "FBD" are the Foiles-Baskes-Daw EAM functions from Ref. 10, and were fitted to the lattice constant, sublimation energy, elastic constants, vacancy-formation energy, a simplified equation of state, and dilute heats of alloying with other fcc metals. "FP-EAM" are the first-principles EAM functions from this work, and were obtained from the TFDvW model, which was adjusted to fit the lattice constant and sublimation energy. (a) Effective two-body interaction in the fcc bulk. (b) Effective three-body interaction of atoms in an equilateral triangle, in the fcc bulk.

EAM functions.

Actually, the interactions in Eqs. (29) allow us to recall that the effective interactions within the EAM are *environment dependent,* in that the interaction between two atoms depends on the slopes of their embedding functions, which depend on the $\bar{\rho}$ for each atom. This, in fact, is the strength of the EAM, and is directly connected to the nonlinearity of the embedding function.

We have therefore plotted in Figs. 6(a) and 6(b) the effective pair and trio interactions for three EAM sets of functions for Ni: the original semiempirical functions developed by Daw and Baskes, the semiempirical functions developed by Foiles, Daw, and Baskes for fcc alloys, and the functions developed in this paper from the TFDvW-model energy functional. The results show that the effective energetics of the three functions are rather similar, and that the semiempirical functions are qualitatively quite similar to what one gets from more fundamental considerations.

In summary, we have developed a model energy functional for nickel and shown that the model gives a reasonable description of the energetics of basic defects. We have then obtained EAM functions from this model and demonstrated that the EAM form can reasonably reproduce the energetics of this functional. We examined the weighting-function solution for the optimum constant background density and found that it is approximately correct, with the error in the solution being most significant for the surface. An improvement to the weighting function solution was proposed, which included corrections due to the derivatives of the background density.

IV. CONCLUSIONS

A simplified expression for the cohesive energy of a solid can be derived from approximations to density-functional theory. The energy can be divided into an embedding-energy contribution with an electrostatic, two-body correction. The procedure defines an optimal constant background density, $\bar{\rho}$, for the embedding function, in terms of the actual background density $\rho_b(r)$ at each site. An approximation to $\bar{\rho}$ is given by a weighted average over $\rho_b(r)$. The weighting function is sufficiently localized that it may be approximated by a δ function, so that $\bar{\rho} \sim \rho_b(0)$, where 0 is the position of the nucleus. Using the Thomas–Fermi–Dirac–von Weizsäcker model for Ni, we have derived a new set of EAM functions from first principles (in contrast to previous semiempirical functions). These new functions reproduce the TFDvW calculation of the energetics of defects of the solid. Within the model, $\bar{\rho}$ was found to be adequately described by $c_1 + c_2\rho_b(0)$, except for the surface. A correction to $\bar{\rho}$ was suggested which involved derivatives of $\rho_b(r)$. The new functions are qualitatively similar to previously obtained semiempirical functions.

The expressions developed here for the EAM can serve as a basis for the parametrization of the functions used in the semiempirical technique.

ACKNOWLEDGMENTS

The author would like to thank Drs. S. M. Foiles and M. I. Baskes of this laboratory for their useful comments. This work was supported by Division of Materials Science, Office of Basic Energy Sciences, of the U.S. Department of Energy.

[1] *Interatomic Potentials and Crystalline Defects,* edited by J. K. Lee (Metallurgical Society of AIME, New York, 1981).

[2] W. A. Harrison, *Pseudopotentials in the Theory of Metals* (Benjamin, New York, 1966).

[3] R. A. Johnson, Phys. Rev. B **6**, 2094 (1972).

[4] See, for example, C. L. Briant and R. P. Messmer, Philos. Mag. B **42**, 569 (1980), or M. I. Baskes, C. F. Melius, and W. D. Wilson, in Ref. 1.

[5] See, for example, T. L. Einstein and J. R. Schrieffer, Phys. Rev. B **7**, 3629 (1983), or A. G. Eguiluz, D. A. Campbell, A. A. Maradudin, and R. F. Wallis, *ibid.* **30**, 5449 (1984), or P. Nordlander and S. Holmstrom, Surf. Sci. **159**, 443 (1985).

[6] M. S. Daw and S. M. Foiles, Phys. Rev. B **35**, 2128 (1987).

[7] M. S. Daw and M. I. Baskes, Phys. Rev. Lett. **50**, 1285 (1983); Phys. Rev. B **29**, 6443 (1984).

[8] M. S. Daw and R. L. Hatcher, Solid State Commun. **56**, 697 (1985).

[9] S. M. Foiles, Phys. Rev. B **32**, 3409 (1985).

[10] S. M. Foiles, M. I. Baskes, and M. S. Daw, Phys. Rev. B **33**, 7983 (1986).

[11] M. S. Daw, M. I. Baskes, C. L. Bisson, and W. G. Wolfer, in *Modeling Environmental Effects on Crack Growth Processes,* edited by R. H. Jones and W. W. Gerberich (The Metallurgical Society, Warrendale, PA, 1986).

[12] M. S. Daw and S. M. Foiles, J. Vac. Sci. Technol. A **4**, 1412 (1986), M. S. Daw, Surf. Sci. **166**, L161 (1986), S. M. Foiles, *ibid.* **191**, L779 (1987).

[13] T. E. Felter, S. M. Foiles, M. S. Daw, and R. H. Stulen, Surf. Sci. **171**, L379 (1986).

[14] S. M. Foiles, Phys. Rev. B **32**, 7685 (1985).

[15] M. S. Daw and S. M. Foiles, Phys. Rev. Lett. **59**, 2756 (1987).

[16] S. M. Foiles, Surf. Sci. **191**, 329 (1987).

[17] J. S. Nelson, E. C. Sowa, and M. S. Daw, Phys. Rev. Lett. **61**, 1977 (1988).

[18] J. K. Nørskov and N. D. Lang, Phys. Rev. B **21**, 2131 (1980).

[19] M. J. Stott and E. Zaremba, Phys. Rev. B **22**, 1564 (1980).

[20] J. K. Nørskov, Phys. Rev. B **26**, 2875 (1982).

[21] P. Nordlander, S. Holloway, and J. K. Nørskov, Surf. Sci. **136**, 59 (1984).

[22] K. W. Jacobsen, J. K. Nørskov, and M. J. Puska, Phys. Rev. B **35**, 7423 (1987).

[23] M. Manninen, Phys. Rev. B **34**, 8486 (1986).

[24] J. D. Kress and A. E. DePristo, J. Chem. Phys. **87**, 4700 (1987); **88**, 2596 (1988).

[25] P. Hohenberg and W. Kohn, Phys. Rev. **136**, B864 (1964).

[26] M. J. Puska, R. M. Nieminen, and M. Manninen, Phys. Rev. B **24**, 3037 (1981).

[27] The approximation is physically reasonable as can be observed by comparing, for example, ϕ^a_{NiCu} and $(\phi^a_{\mathrm{NiNi}}\phi^a_{\mathrm{CuCu}})^{1/2}$ from Eq. (26).

[28] J. R. Chelikowsky, Solid State Commun. **31**, 19 (1979); Phys. Rev. B **21**, 3074 (1980).

[29] D. Pines, *Elementary Excitations in Solids* (Benjamin,New York, 1964).

[30]C. V. von Weizsäcker, Z. Phys. **96**, 431 (1935).
[31]W. Jones and N. H. March, *Theoretical Solid State Physics* (Wiley-Interscience, New York, 1973), Vol. 1, p. 200.
[32]W. Jones and W. H. Young, J. Phys. C **4**, 1322 (1971).
[33]E. Clementi and C. Roetti, *Atomic Data and Nuclear Data Tables* (Academic, New York, 1974), Vol. 14, Nos. 3 and 4.
[34]C. S. Barrett and T. B. Massalski, *Structure of Metals* (McGraw-Hill, New York, 1966).
[35]*Metal Reference Book,* 5th ed., edited by C. J. Smith (Butterworths, London, 1976), p. 186.
[36]V. L. Moruzzi, J. F. Janak, and A. R. Williams, *Calculated Electronic Properties of Metals* (Pergamon, New York, 1978).
[37]G. Simmons and H. Wang, *Single Crystal Elastic Constants and Calculated Aggregate Properties: A Handbook* (MIT, Cambridge, MA, 1971).
[38]W. Wycisk and M. Feller-Kniepmeier, J. Nucl. Mater. **69&70**, 616 (1978).
[39]H. Kronmuller, in *Vacancies and Interstitials in Metals,* edited by A. Seeger, D. Schumacher, W. Schilling, and J. Diehl (North-Holland, Amsterdam, 1970), p. 183.
[40]W. R. Tyson and W. A. Miller, Surf. Sci. **62**, 267 (1977).
[41]*Computer Calculation of Phase Diagrams,* edited by L. Kaufman and H. Bernstein (Academic, New York, 1970).